Applied Energy 247 (2019) 492–502

Contents lists available at ScienceDirect

Applied Energy

journal homepage: www.elsevier.com/locate/apenergy

Active harvesting enhances energy recovery and function of electroactive microbiomes in microbial fuel cells

Lu Lu[a,1], Fernanda Leite Lobo[b,1], Defeng Xing[c,*], Zhiyong Jason Ren[a,b,*]

[a] Department of Civil and Environmental Engineering and Andlinger Center for Energy and the Environment, Princeton University, Princeton, NJ 08544, United States
[b] Department of Civil, Environmental, and Architectural Engineering, University of Colorado Boulder, Boulder, CO 80309, United States
[c] School of Environment, State Key Laboratory of Urban Water Resource and Environment, Harbin Institute of Technology, Harbin 150090, China

HIGHLIGHTS

- Active harvesting significantly enhanced MFC performance for energy recovery.
- Active harvesting shaped anode microbiomes towards more electrochemically efficient.
- Active harvesting promoted more abundant *Geobacter* and c-type cytochrome genes.
- Metagenomics provided more accurate and completed information than marker gene.

GRAPHICAL ABSTRACT

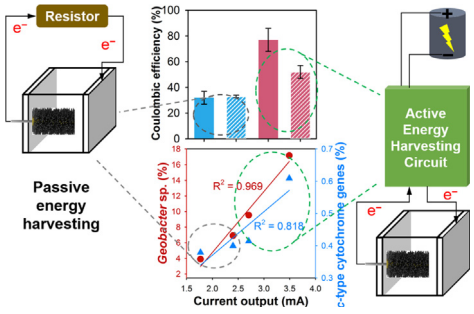

ARTICLE INFO

Keywords:
Microbial electrochemical technology
Microbial fuel cell
Active energy-harvesting
Microbial community
Metagenomics
Wastewater treatment

ABSTRACT

The performance of microbial fuel cells in terms of current production and waste removal depends on microbial electron transfer catalyzed by functional communities. Active energy harvesting using tunable electrical circuits in this study dramatically increased microbial fuel cell performance compared with passive harvesting using resistors. Operated under four different conditions under either high power or high current, active harvesting increased power output by up to 240%, current output by 45%, and Coulombic efficiency by 141%. Moreover, the dynamic harvesting created a selective pressure on the anodic biofilm and greatly shaped the microbial community and function. It promoted the enrichment of electroactive bacteria with higher efficiency of electron transfer and thereby improved reactor performance. Using both marker gene sequencing and metagenomics tools, the study revealed distinct clusters of microbial community on the anodic biofilm under different harvesting conditions, and the abundance of known electroactive bacteria *Geobacter* more than tripled in active harvesting condition. Similar trends were discovered in the increased abundance of *c*-type cytochrome genes associated with extracellular electron transfer. Statistical analysis showed strong positive correlations between the abundance of functional genes and electrochemical performance of reactors. Compared with 16S rRNA marker gene methods that only examine the general microbial community structure, metagenomics used here revealed more accurate structure information as well as the functions of microbial community.

* Corresponding authors at: Department of Civil and Environmental Engineering and Andlinger Center for Energy and the Environment, Princeton University, Princeton, NJ 08544, United States (Z.J. Ren).
E-mail addresses: lu.lu@princeton.edu (L. Lu), Fernanda.lobo@colorado.edu (F.L. Lobo), dxing@hit.edu.cn (D. Xing), zjren@princeton.edu (Z.J. Ren).
[1] These authors contributed equally to this work.

https://doi.org/10.1016/j.apenergy.2019.04.074
Received 26 December 2018; Received in revised form 20 March 2019; Accepted 15 April 2019

1. Introduction

The economic, environmental and social impacts of fossil fuel exploration, production and consumption are driving the development of renewable energy alternatives, but to replace fossil fuels a variety of energy sources are needed to meet different needs. The microbial electrochemical technology (MET) has been intensively researched in recent years as a clean, distributed and renewable energy technology, because it offers a simple and direct method for converting the chemical energy embedded in biomass (e.g. wastewater) into other forms of energy, such electrical energy and hydrogen energy, while at the same time achieving environmental cleanup goals [1,2]. The core uniqueness of MET process comes from the electroactive bacteria (EAB) used in these systems. Such microbes are capable of degrading organic substrates to transfer electrons of anaerobic respiration to the anode to form current [3,4]. Despite recent advancements on materials, reactor configurations and operations, the energy output of MET is still low, which is not sufficient for real world applications [5,6].

The performance of an MET is directly related to the efficiency of energy harvesting from organics by a bioanode regardless the end use of energy for current production (microbial fuel cell), H_2 production (microbial electrolysis cell), desalination (microbial desalination cell) or chemicals generation (microbial electrosynthesis) [7,8]. Taking microbial fuel cell (MFC), a classic MET, as an example, it conventionally operated at a fix load, such as a resistor or charge pump, to recover electrical energy. This process allows electrons to passively pass through the circuit without generating any feedback to the microorganisms [9], so it is considered as a passive process for energy harvesting [6]. To examine how to improve energy efficiency of MFC bioanodes, the common practice is control of the bioanode potential based on the thermodynamic assumption that EAB could obtain more energy when final electron acceptor (anode) has a higher redox potential, as long as microorganisms can generate enough proton motive force [10]. These studies have tried to find a best potential range, where EAB had the highest electroactivity but can still tolerate the high potential [10,11]. However, opposite results were reported by different studies even using the same substrate. For example, Zhu et al., has reported a positive correlation between maximum current and bioanode potentials in the range of −0.25 to 0.21 V [12], while another study demonstrated an obvious reduction of current with bioanode potential increased from −0.15 to 0.37 V [11]. Artificial control of the bioanode potential using expensive potentiostat can only be used in a lab setting but not engineering application. Plus, a fixed anode potential can't give a timely response to a dynamic MFC under constant changes of microbial activities and operational parameters. Emerging active energy harvesting using an electrical circuit is more feasible for real world applications [6]. For example, maximum power point (MPP) tracking was developed for active energy harvesting from the bioanode, which was reported increased energy recovery and coulombic efficiency by 76 and 21 times than a passive charge pump, respectively [13]. MPP tracking circuit was able to maintain MFC output at its peak power point in real time by using pulsed energy tracking and capturing for maximizing the power output. Not only for MPP, active harvesting can also track and adjust harvesting in real time to meet other desired operating points, such as the maximum current point (MCP) [14].

Although active harvesting technologies have been showed to enhance MFC energy output, there is no information on how they shape microbial community structure and functions [6,13,15,16]. The dynamic energy harvesting approach is hypothesized to dramatically shape microbial ecology and metabolisms, because it creates a selective pressure on the microbial community to regulate respiratory pathways for more efficient electron transfer and ATP synthesis [3], yet little fundamental mechanisms of active harvesting are known to connect microbial ecology with electrical energy harvesting and reactor performance. Studies on anode potential control tried to establish a relationship between electroactive microbial community and the bioanode potential, but how did different potentials affect the community structure was not clear and under debate [10,12]. These studies were limited by the 16S rRNA marker gene-based analytical approach, which can only provide community structure information but without function information. Moreover, marker gene sequencing is susceptible to biases that are inherent in gene amplification. This may lead to skewed information about community structure [17,18]. Although some studies have tried to use electrochemical approaches, such as cyclic voltammetry (CV) to deduce community function, direct biological proofs associated with community function are not available.

In this study, we characterized for the first time how active harvesting greatly increased energy output from MFC reactors, and more interestingly how such performance improvement was a result of the shift of microbial community structure and function under the active harvesting environment. Both active harvesting and passive resistor loads were used to provide high power or high current conditions using the same substrate and inoculum. In addition to traditional 16S rRNA gene analysis for the evaluation of microbiomes from bioanode, cathode and electrolyte, shotgun metagenomics was used to further investigate the function of electroactive microbial communities. Metagenomics surveys can capture more phylogenetic information than 16S sequencing, such as rare or novel organisms and identification of specific species, and it can also provide the direct information regarding functional pathways of the targeted microorganisms.

2. Materials and methods

2.1. Reactor construction and operation

Cubic single-chamber MFCs were constructed using polycarbonate, and the empty volume of each MFC chamber was 28 mL. Each MFC reactor contained a heat-treated carbon fiber brush as the anode and a carbon cloth air-cathode (7 cm^2, Fuel Cell Earth) with manufacturing procedure described in previous studies [19,20]. Brewery wastewater obtained from a local brewery (Boulder, CO) was diluted (1:10) by a 50 mM phosphate buffer solution (PBS, $NaH_2PO_4{\cdot}2H_2O$ 3.32 g/L; $Na_2HPO_4{\cdot}12H_2O$ 10.32 g/L; NH_4Cl 0.31 g/L; KCl 0.13 g/L) and was used as the sole substrate during the experiment [21]. The final wastewater contains 1,800 mg/L chemical oxygen demand (COD), 938 mg/L total Kjeldahl nitrogen (TKN), 1860 mg/L phosphate and 70 mg/L potassium. Anaerobic sludge obtained from a local wastewater water treatment plant (Boulder CO, U.S.) was used as the inoculum. Before using, raw sludge was added into the PBS diluted brewery wastewater to form a mixture with the sludge concentration of around 200 mg/L MLVSS (mixed liquor volatile suspended solids). The mixed liquid was fed to the MFCs that were operated in batch mode using a fixed 1000 Ω resistor as the load at room temperature. Once the voltage over the resistor is higher than 100 mV during a batch cycle, the sludge (inoculum) was omitted, and only the fresh wastewater was fed to the reactors.

All reactors were first enriched till repeatable voltage profiles were obtained after 10 days. This short acclimation was only designed for enrichment of bioanode rather than a long-term pre-selection of bacteria that has been done in our previous study [14]. After that, linear sweeping voltammetry (LSV) with a 1 mV/s scan rate was performed on each reactor to determine the key operating points of maximum current points and maximum power points [22]. The total of 8 reactors were then divided into 4 groups, with each group containing duplicate reactors operated in 1 of the 4 following scenarios: maximum current with passive resistor (CR), maximum power with passive resistor (PR), maximum current with active energy harvesting (CH), and maximum power with active energy harvesting (PH). The scenarios can be further divided into 2 groups: active, where the MFC was connected to an energy harvesting circuit being controlled to track maximum power (PH) or current (CH), and the MFC energy was used to charge a battery [13,14]; and passive, where resistor with values that would achieve

maximum power (PR) or current (CR) were connected in parallel with the MFC, but the MFC energy could only be dissipated as heat. The abbreviations of the different scenarios and important definitions are summarized in Table S1.

For active harvesting scenarios, the circuits were controlled to track maximum power (PH) or maximum current (CH) by operating voltages that were determined using the LSV results mentioned above. The LSV results were used to identify the maximum power point and correlate this point with a voltage, V_{MPP} (maximum power point voltage). Hence, the MFCs running on PH mode would be controlled to have a constant voltage at V_{MPP} using an integrated energy harvesting nano-power management circuit with pulse-frequency modulated (PFM) boost converter/charger (bq25505, Texas Instruments Inc.) [14]. Since the maximum current would be given at 0 V, an approximation of V_{MCP} (maximum current point voltage) between 80 mV and 100 mV was used to give the highest possible controlled current by the circuit, which was 85% of the short circuit current. A programmable maximum power point tracking (MPPT) unit is embedded in the circuit and keeps sampling the open circuit input voltage every 16 s and calculates V_{MPP} as 50% or 80% of the open circuit voltage. In this study, because on MFCs, the open circuit voltage takes more than a few seconds to reach its real value, the programmable MPPT was set using a reference voltage at either V_{MPP} or V_{MCP} from LSV results, and this control was able to maintain a constant MFC voltage on the desired point of the power density curve. The energy extracted from each MFC was stored in polymer lithium ion batteries (840mAh, SparkFun Electronics®).

For the passive energy harvesting conditions, the LSV results were used to identify the maximum power point and correlate this point with a voltage (V_{MPP}) and current (I_{MPP}), so the resistor value could be calculated ($R_{MPP} = V_{MPP}/I_{MPP}$). The maximum current point was determined to be at 85% of the short circuit current to be comparable to CH scenario, and the resistor value was calculated using the maximum current point voltage (V_{MCP}) and current (I_{MCP}).

2.2. Chemical analyses

The individual potential of each anode and cathode was measured at each batch using Ag/AgCl reference electrodes (RE-5B, +0.210 V versus standard hydrogen electrode, 25 °C). Reactor voltages were recorded using a data acquisition system (Keithley, OH). Cyclic voltammetry (CV) was performed before and after batch operations in different stages. The potential range for CV was determined as −0.7 to 0 V vs. Ag/AgCl with a scan rate 1 mV/s based on previous results [23]. First derivative CV (DCV) was derived from turnover CV to determine the changes in each peak value. The main oxidation peak in DCV was fitted to Guassian function to separate overlapped peaks. LSV tests were performed using the same potentiostat with a scan rate of 1 mV/s with either the anode or the cathode as the working electrode, depending on characterization purposes. Chemical oxygen demand (COD) before and after each batch was measured using the standard method with a spectrophotometer (DR 3900, Hach Co., Loveland, CO, USA). Coulombic efficiency (CE) was determined using Eq. (1), where $M = 32$ (molecular weight of oxygen), F is faraday constant, $b = 4$ is the number of electrons exchanged per mole of oxygen, v_{an} is the liquid volume of anode compartment, and ΔCOD is the change in COD over time [9,24].

$$CE = \frac{M \int_0^t Idt}{Fbv_{an}\Delta COD} \quad (1)$$

2.3. DNA extraction

Genomic DNA extraction was performed on day 60 and 90 after operation. Anode biofilm (Fig. S11) was collected by cutting small pieces of carbon fiber from at least five different locations on the anode and then fragmented them using a sterile scissor. Visible cathode biofilm was directly collected from cathode surface using a sterile knife. Microorganisms in electrolyte were collected by filtering solution using a sterile membrane with a pore size of 0.22 μm. Total genomic DNA of all samples was extracted using a PowerSoil DNA Isolation Kit (MoBio Laboratories, Inc., Carlsbad, CA) according to the manufacturer's instructions.

2.4. 16S rRNA gene-based analysis of microbial community structure

The V4 region of the bacterial/archaeal 16S rRNA gene was targeted using a nucleotide barcoded forward primer 515F 5′-GTGCCAGCMGCCGCGG-3′ and the reverse primer 907R 5′-CCGTCAATTCMTTTRAGTTT-3′. High-throughput sequencing of the PCR amplicons was performed on an Illumina Miseq PE 250 platform. After quality control, 48 samples generated a total of 1803,530 high-quality 16S rRNA gene sequences with an average length of 375 bp, which were assigned into 619 OTUs with a distance limit of 0.03. Good's Coverage estimators indicate that a highly sufficient coverage (99.7 ~ %) of the microbial communities by the libraries. The biodiversity indices, such as Shannon index (H') including information of both richness and evenness of species were provided in Supplementary material Table S2. QIIME pipeline was used for microbial community structure analysis, briefly, including processes of demultiplexing and quality filtering of raw sequences, OTU and representative sequences picking, taxonomic assignment, phylogenetic reconstruction, and alpha (e.g. Chao, Ace, coverage, simpson indices) and beta (e.g. weighted UniFrac) diversity analyses [25]. Raw sequencing data were deposited to the NCBI Sequence Read Archive (SRA) with accession No. SRP174552.

2.5. Shotgun metagenomics analysis

Illumina shotgun DNA library construction & sequencing were performed by Biozeron Biotechnology Co., Ltd at Shanghai, China. Briefly, after fragmentation, indexed paired-end DNA library was prepared using TruSeq DNA Sample Prep Kit, then the cluster generation was conducted using a TruSeq PE Cluster Kit v3-cBot-Hs. Fragments were sequenced on the Illumina HiSeq 2000 platform using a TruSeq SBS Kit v3-HS (200 cycles). Software Seqprep (https://github.com/jstjohn/SeqPrep) and Sickle (https://github.com/najoshi/sickle) were used for reads quality control, such as adapter removal, trimming of 3′-end or 5′-end of reads with incorrectly called bases, elimination of trimmed reads with length shorter than 50 bp, and quality value lower than 20, etc. The sequences were deposited to the Metagenomics RAST (MGRAST)

sever with accession numbers mgm4827784.3 and mgm4829787.3-4829793.3.

The valid sequences reads were assembled into contigs using a De-Brujin graph based software SOAPdenovo (http://soap.genomics.org.cn/, Version 1.06) with a range of k-mer values of 39–47. The statistics of assembly results was provided in Table S3. MetaGene software (http://metagene.cb.k.u-tokyo.ac.jp/) was used to predict open reading frames (ORFs) from contigs with statistics of predicted results provided in Table S4. Predicted ORFs with length longer than 100 nt were translated into protein sequences. Software CD-HIT (http://www.bioinformatics.org/cd-hit/) was used to remove "redundant" (or highly similar) sequences (95% identity and 90% coverage) to generate a "non-redundant" gene catalog. High quality reads of each samples were mapped back to the "non-redundant" gene catalog (95% identity) to determine gene abundance among the sample using a software of SOAPaligner (http://soap.genomics.org.cn/). Taxonomic classification of reads was conducted by aligning translated protein sequences to the NCBI-NR database with an e-value of 10^{-5} using BLASTP software (BLAST Version 2.2.28+, http://blast.ncbi.nlm.nih.gov/Blast.cgi). Functional annotation of the "non-redundant" gene catalog was performed using BLASTP against the database of eggNOG (http://

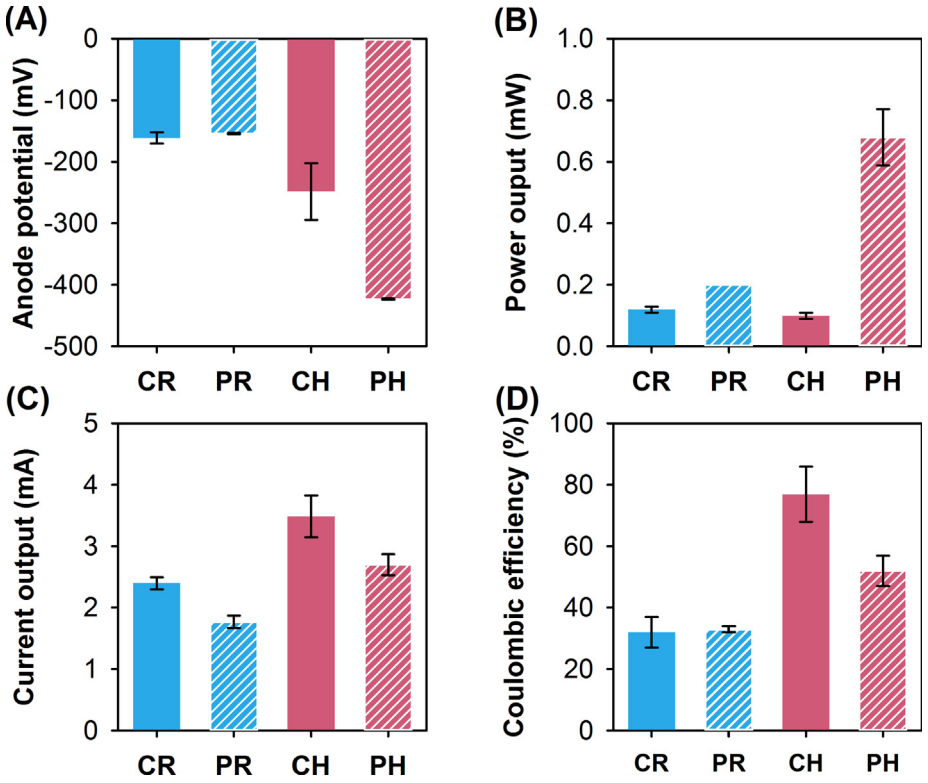

Fig. 1. (A) Average anode potential, (B) stable power and (C) current output, (D) Coulombic efficiency, of MFCs under four harvesting scenarios: maximum current (CR) and power (PR) using resistor as well as maximum current (CH) and power (PH) using active energy-harvesting circuit.

eggnogdb.embl.de/) and KEGG (https://www.genome.jp/kegg/) to obtain COG (Cluster of orthologous groups of proteins) and KEGG Orthologs (KO), respectively, with an e-value of 10^{-5}. COG and KEGG entries with standard deviation in top 100 were normalized to z-score relative abundance, and then were clustered and heatmap plotted using Genesis software.

3. Results and discussion

3.1. Energy harvesting significantly boosted MFC performance

Fig. 1 compared the average anode potential, stable power and current output, and Coulombic efficiency for reactors operated in 4 different conditions. While CR and PR showed similar average anode potential (-164 ± 9 mV and -154 ± 1 mV vs. Ag/AgCl reference electrode, respectively), reactors under active energy harvesting showed much lower anode potential, with CH at -248 ± 46 mV and PH at -423 ± 1 mV, respectively (Fig. 1A). In addition, active energy harvesting generated 50% higher current than those operated in external resistors mode (Fig. 1C). These results indicated that active harvesting significantly reduced the overpotential of reactions occurred on the bioanode. Because a theoretical potential of acetate oxidation on the bioanode is around -490 mV [9], polarization of anode under higher current would theoretically lead to a positive shift of anode potential, that is, overpotential generation. Overpotential reduction by active harvesting means less energy losses and may be attributed to improvement of biofilm electron transfer. A previous study showed that a high current is necessary to maintain the long-term viability of both inner- (near the anode surface) and outer-layer electroactive biofilms [26], which in turn will facilitate electron transfer. Although an accumulation of dead cells within inner-layer biofilm will not affect electron transfer between electrode and biofilm as dead layer may function as an electrically conductive matrix, this will increase a resistance of electron-mediator diffusion [27]. In terms of power output, PH stands out by producing a highest power of 0.68 ± 0.09 mW (Fig. 1B), which is multiple times higher than other operational conditions including that has the similar maximum power scenario but using passive approach (RH). Similarly, active harvesting mode led to much higher Coulombic efficiency. The CH reactor obtained the highest Coulombic efficiency $77 \pm 9\%$, which is followed by PH ($52 \pm 5\%$), while CR and PR only obtained efficiencies around 32% (Fig. 1D). This is exciting as it means a higher conversion efficiency from organic substrate to electricity as well as faster wastewater treatment. Time course profiles (Fig. S1 and S2) showed the current output by active harvesting was stable and highly repeatable. During a same operating period, active processes demonstrated more fed-batch cycles than that of passive scenarios, indicating they have the higher efficiencies of wastewater treatment. Plus, PH and CH reactors were able to store the electrical energy in rechargeable batteries while no real energy was stored in PR and CR reactors as it was dissipated as heat on the resistor. All these results indicated that the active harvesting are promising strategies to recover energy in real applications.

3.2. Electrochemical responses characterized by cyclic voltammetry

Fig. 2 shows the profiles of cyclic voltammetry (CV) of the reactors operated under four scenarios on day 30, 40, 50, 70, 80, and 90. The CH reactors that demonstrated the highest electroactive bacteria activities showed a maximum current of 12.48 ± 0.7 mA, nearly doubled the current obtained in PR reactors (6.75 ± 0.3 mA) (Fig. 2A and B). This is expected as CH operation is designed to extract more electrons to the anode. The bioanodes midpoint potentials didn't shift over the 90-day of operation, but an obvious current drop was observed after 50 days due to the decay of air cathode. Air-cathode biofouling has been known as an issue in long term MFC operation [28]. Reactor midpoint potentials in energy harvesting reactors (PH and CH) were at the same low level (around 414 mV vs. Ag/AgCl) (Fig. 2C). Because a mixed culture of microorganisms was used, the electroactive cytochromes involved in

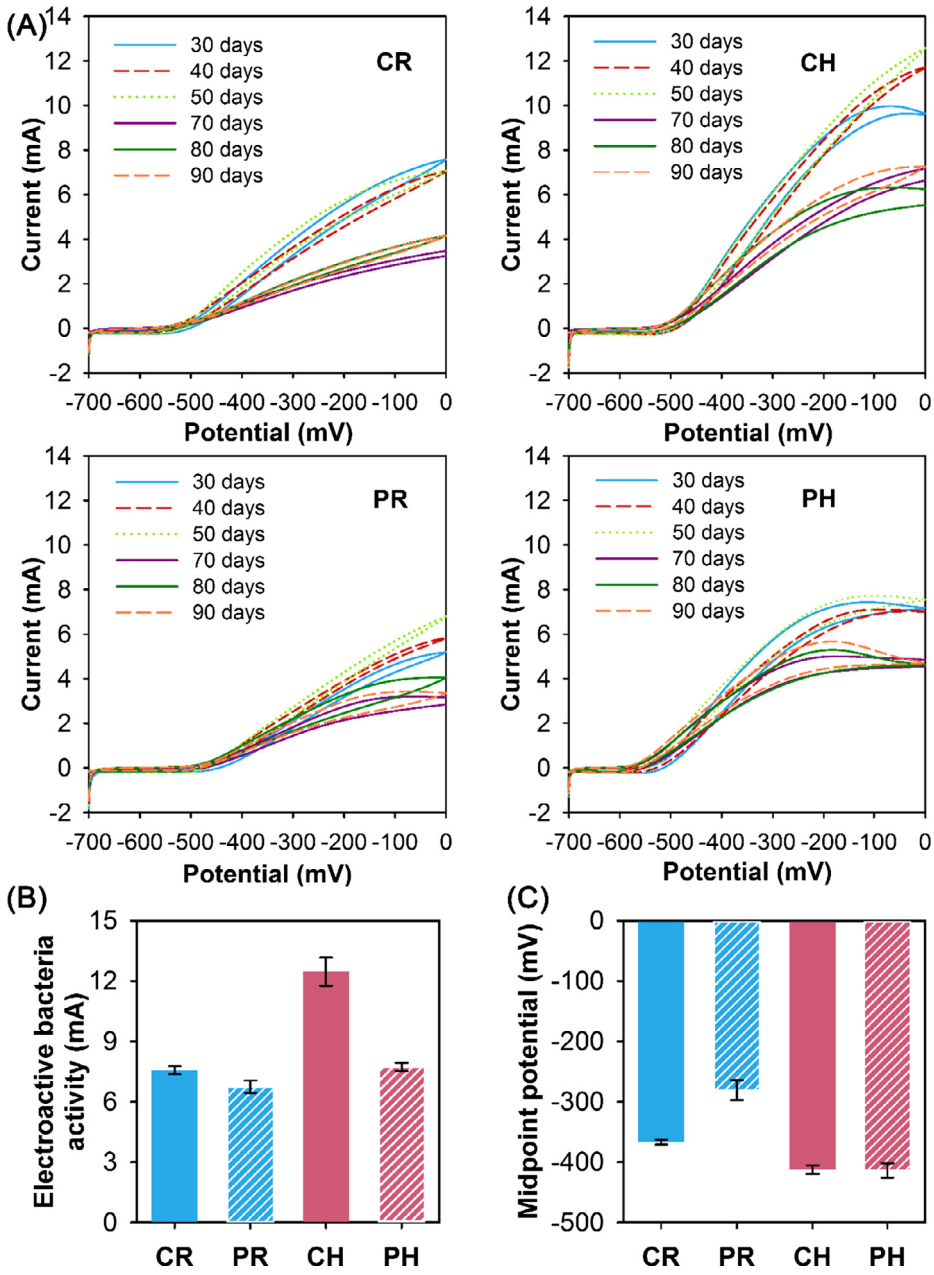

Fig. 2. (A) Cyclic voltammetry (CV) profiles on day 30, 40, 50, 70, 80, and 90 of reactors running at maximum current (CR) and power (PR) using resistor as well as maximum current (CH) and power (PH) using active energy-harvesting circuit. Statistics of (B) electroactive bacteria activity showed as a maximum current on CV curve, and (C) midpoint potential of bioanodes.

extracellular electron transfer were mixed and difficult to be identified, but this low midpoint potential was discussed in previous studies similar as multiple cytochromes *OmcZ, OmcS* and *OmcB* [29]. The CR reactor showed a midpoint potential of −367 ± 4 mV, which is close to the potential of *PpcA cytochromes* [30]. In contrast, PR operation led to the highest midpoint potential of −281 ± 17 mV, which was rather close to the potential of some known electron shuttles like ACQN quinones (−281 mV) and pycyanine phenazines (−310 mV) [29]. However, even though the electrochemical results show an interesting trend, it is difficult to directly connect the midpoint potentials and CV profiles with specific microbial community structure and function. Because mixed microbial culture used here was more complicated compared with a pure culture. Direct biological investigation is needed by employing culture-independent approaches, such as marker gene sequencing and metagenomics.

3.3. Overall distinction of microbial community under different energy-harvesting scenarios

To reveal the impacts of active energy harvesting on microbial communities, both high-throughput culture-independent 16S rRNA gene sequencing and shotgun metagenomics were used to identify the different microbial communities from the anode, cathode and electrolyte in MFCs under different energy harvesting scenarios (Fig. 3). Multiple samples were taken from duplicate reactors in different stages of operation (60 days and 90 days) to provide statistical and dynamic data analysis of microbial communities that responded to the selective pressure posed by active harvesting. Very interestingly, distinct clusters of anode microbial communities were found under different energy harvesting conditions by 16S rRNA gene-based Weighted Fast UniFrac Principal Coordinates Analysis (PCoA) (Fig. 3A). The anode biofilm samples are distributed into four distinct and separated clusters based

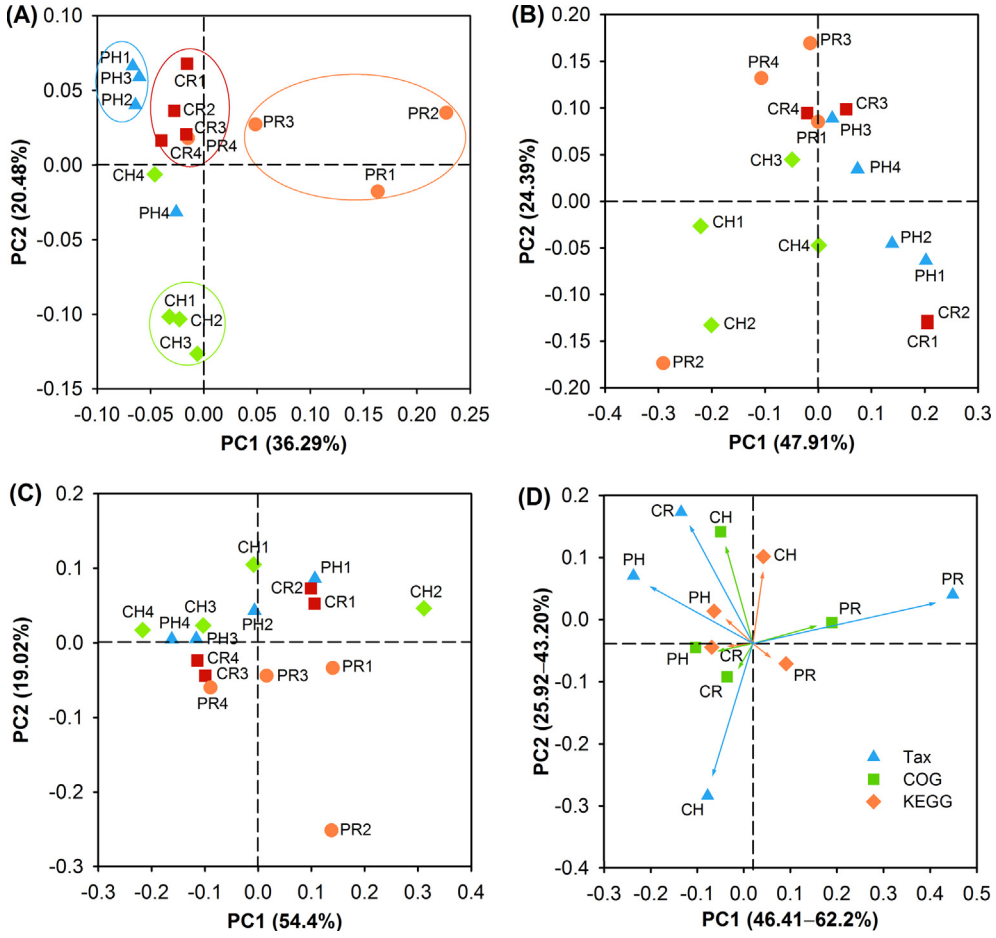

Fig. 3. Weighted Fast UniFrac Principal Coordinates Analysis (PCoA) of the microbial communities of (A) anode biofilms, (B) cathode biofilms, and (C) electrolyte in MFCs on the basis of 16S rRNA gene as well as (D) metagenomic based PCoA of anode biofilms collected on day 60 with tax, COG and KEGG annotation. Reactors were operated at maximum current (CR) and power (PR) using resistor as well as maximum current (CH) and power (PH) using active energy-harvesting circuit. The characters of "1" and "2" in abbreviations of samples indicate duplicate samples collected on day 60, and "3" and "4" indicate duplicate samples collected on day 90.

on each harvesting scenario as shown in Fig. 3A. The microbial community structure associated with CH (green) is very distant from the communities in other scenarios. This is related to the results that CH operation showed the highest current production and Coulombic efficiency. PH (blue) and CR (red) clusters are close to each other, and they also showed comparable current outputs (2.71 ± 0.17 mA and 2.4 ± 0.1 mA, respectively) (Fig. 1C). The community structure associated with the PR (orange) is dispersed and distant from other scenarios, and correspondingly the PR reactors had the lowest current production and Coulombic efficiency. The almost identical results as marker gene analysis were obtained from metagenomic analysis of microbial communities based on both structure and function (Fig. 3D). These findings solidly supported that even using the same substrate and microbial inoculum, the active energy harvesting shaped the MFC anode microbial communities that were drastically different from passive energy harvesting. The anode potentials of reactors under active harvesting were far lower than passive operations (Fig. 1A), indicating a direct correlation with the microbial community. This clear up some of the previous confusions that whether anode potentials influence anode community. For example, several studies indicated direct influence regardless of the type of substrates [10,11,31,32], but one study found no influence was observed when using acetate [12].

In contrast, less clear distribution is found in cathode communities despite four separated clusters could be identified based on each harvesting scenario a) CH1 and CH2; b) PH1 and PH2; c) CR1 and CR2; and d) PR3 and PR4. The microbial community in solution samples are all mixed together without an identifiable trend (Fig. 3C). Previous study has showed that electrolyte associated community composition was also influenced by anode potential using non-fermentable mixed volatile fatty acids (VFAs) as substrate [10]. In this study, fermentable substrates, such as carbohydrates, are abundant in real wastewater, where fermentative bacteria dominated in all electrolytes with a role of breaking down sugars into acids and other fermentation products. Fermentative bacteria are expected with less impact by electrode compared to electroactive bacteria using VFAs.

3.4. Taxonomic structure and functional profile reveals increased abundance of Geobacter

16S rRNA gene-based sequencing showed that eight microbial phyla including one archaeal phylum and seven bacterial phyla were dominant in MFCs (Fig. 4A). The most sequences on the anode belonged to *Bacteroidetes* (27–40%), *Firmicutes* (18–37%) and *Proteobacteria* (14–44%). The cathode and solution communities mainly consisted of *Bacteroidetes* (9–44%) and *Proteobacteria* (24–91%). This microbial distribution is similar as previous MFC studies in treating brewery wastewater [33,34]. Both 16S rRNA gene and metagenomic analyses indicated that the phylum composition of anode communities was relative stable with time of reactor operation under each scenario (Fig. 4A and 5A). However, *Firmicutes* abundance in the cathode biofilm and electrolyte at two sampling points (day 60 and 90) were found with high variety. *Firmicutes* are generally related to fermentation and possible electroactivity in MFC [35,36]. These results indicate that *Firmicutes* in the microbial communities of cathode and electrolyte may be more susceptible to the electrochemical selective pressure compared to that on the anode. Interestingly, there is a discrepancy about the *Firmicutes* abundance on the anode based on different analysis approaches, for example, metagenomics demonstrated a lower abundance (14–17%) than that of 16S rRNA gene (18–37%), indicating multiple culture-independent approaches are necessary in one study to avoid errors

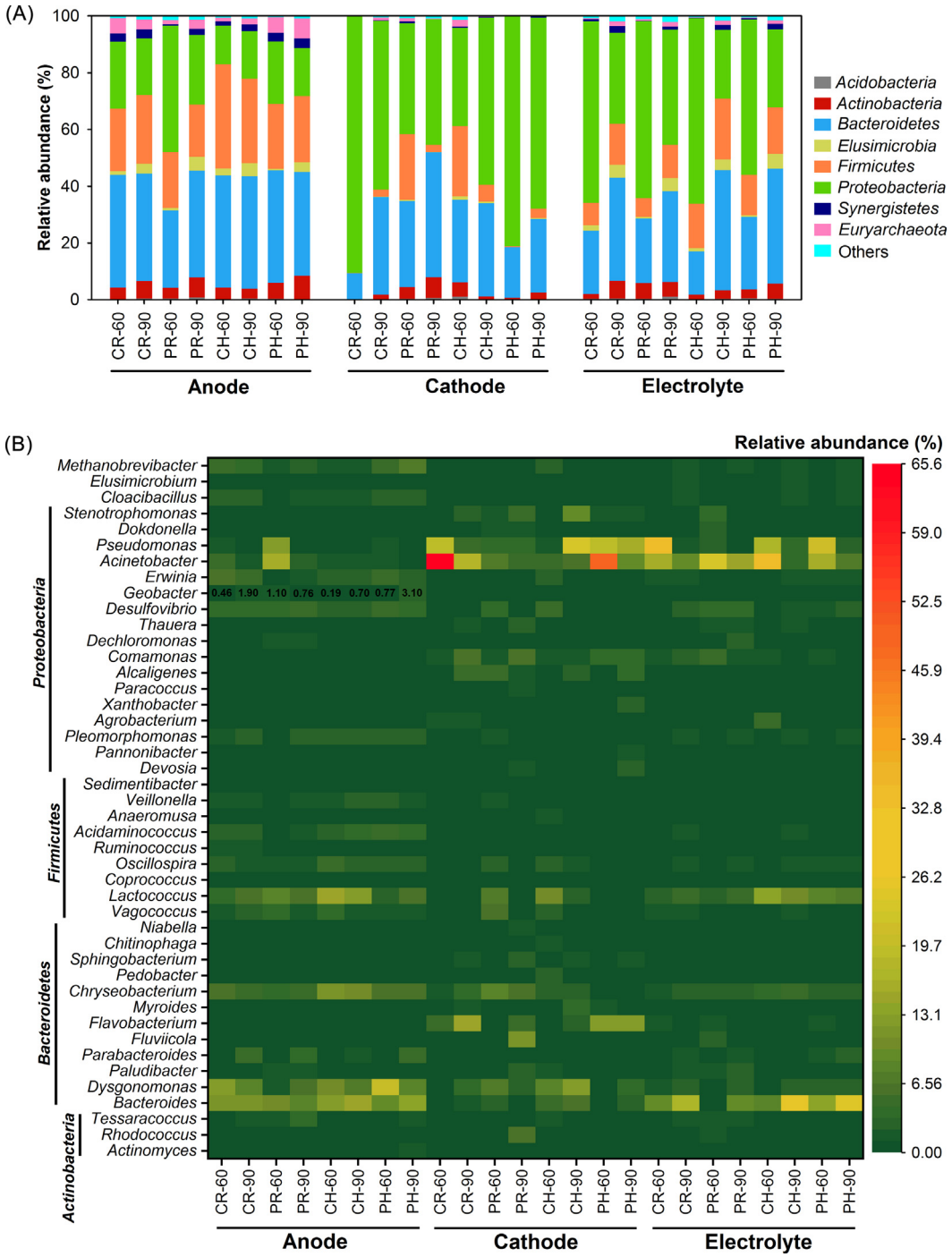

Fig. 4. Taxonomic classification of 16S rRNA gene sequences at (A) phylum level (unranked phyla and phyla that are less than 1% abundance in all libraries were classified as Others) and (B) the most dominant genus level distribution (genera that are less than 1% abundance in all libraries were ignored). Reactors were operated at maximum current (CR) and power (PR) using resistor as well as maximum current (CH) and power (PH) using active energy harvesting circuit. The characters of "60" and "90" in abbreviations of samples indicate samples collected on day 60, and 90. The sequences obtained from duplicate reactors at the same sampling time were combined for bioinformatic analysis.

produced by methodology. Archaeal phylum *Euryarchaeota* was found more abundant on the anode compared to cathode and catholyte. The frequent replacement of electrolyte with short retention time maybe the reason to keep their concentration low in the electrolyte, and the microaerobic environment on the cathode also inhibited their growth.

The genus level characterization further illustrates the difference and diversity of the functional communities. Fig. 4B presents a heat map that shows the relative abundance of different bacteria genera found in different samples based on the 16S rRNA gene. *Bacteroides* and *Dysgonomonas* were found abundant in all anode samples. They are known as fermentative bacteria for sugar catabolism with major products of hydrogen and lower fatty acids such as acetate and succinate [37]. Because almost all known electroactive bacteria (EAB) utilize simple volatile fatty acids or alcohols for electricity generation, it is reasonable to hypothesize that the quick consumption of these fermentation products facilitated fermentation process of brewery wastewater and therefore led to higher abundance of fermentative bacteria on the anodes. Cathode and electrolyte samples showed relatively

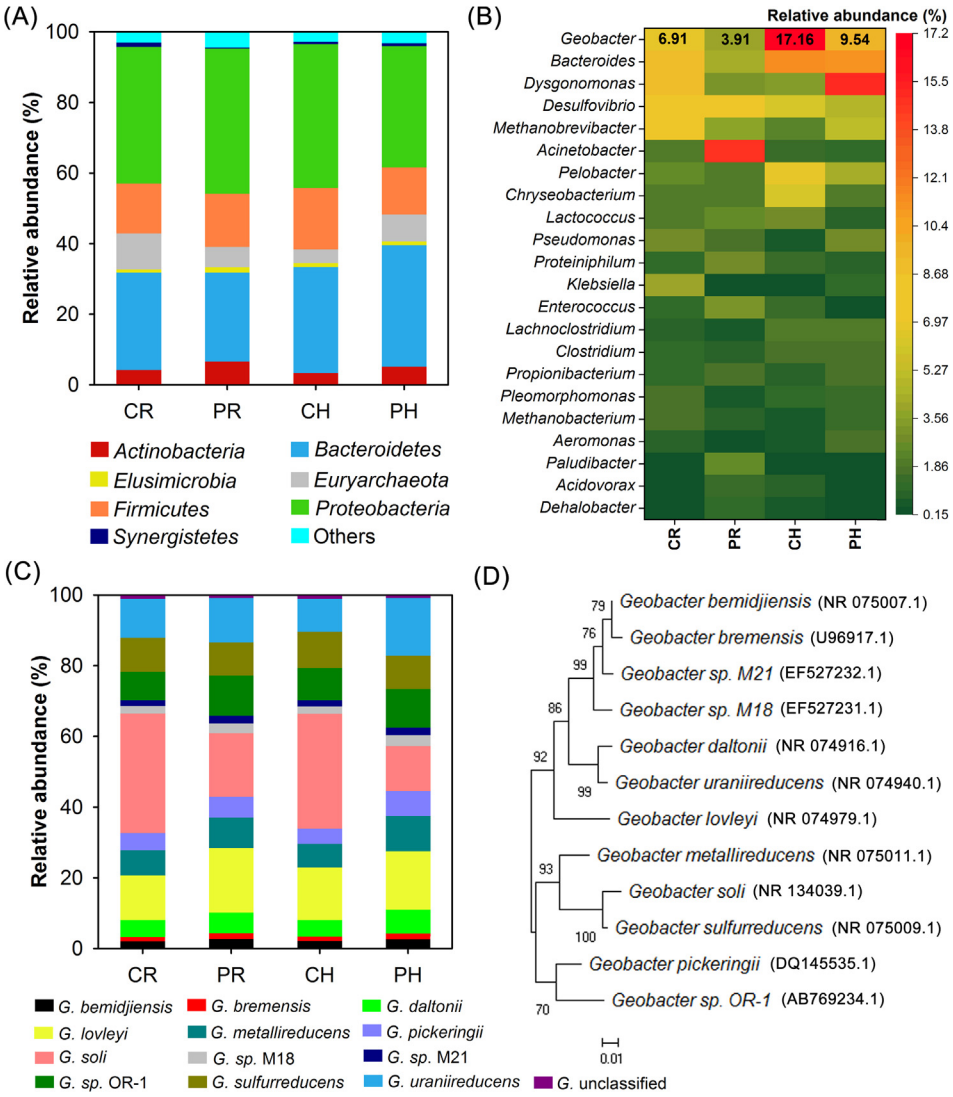

Fig. 5. Metagenomic insights into the dominant microbial (A) phylum and (B) genus, and (C) species level distribution of genus *Geobacter* and their phylogenetic tree in bioanode communities collected on day 60 under maximum current (CR) and power (PR) using resistor as well as maximum current (CH) and power (PH) using active energy harvesting circuit.

higher abundance of facultative bacteria *Pseudomonas* and *Acinetobacter*. Although some of these species showed capability of direct or indirect extracellular electron transfer in MFCs [3,38–41], 16S rRNA gene identification is not capable of providing accurate species information due to its limited length of sequences (300–400 bp). Possible EAB *Desulfovibrio* was found with higher abundance on the anode than that of cathode and electrolyte. Hydrogenotrophic methanogens *Methanobrevibacter* was the most abundant archaea genus and dominated on the anodes (Fig. S7-S10), indicating they compete with EAB for substrate H_2. It is also interesting that typical EAB *Geobacter* (~3.1%) were not found dominant in any of the anodes, but its abundance in active harvesting reactors was more than tripled (0.7–3.1%) than those reactors operated under passive harvesting (0.19–0.77%). Moreover, *Geobacter* abundance always increased with operation time among active scenarios while its abundance in passive systems decreased (Fig. 4A), indicating the formation of a selective pressure for EAB enrichment by active harvesting. Reported studies based on 16S rRNA gene usually showed that the abundance of *Geobacter* in MFCs was impacted by the substrates. For example, *Geobacter* spp. were found dominant using non-fermentable substrates [3,42] but were absent when using fermentative substrates [43]. Based on these results, some studies argued that the absolute abundance of *Geobacter* in biofilms cannot be necessarily assumed a priori to correlate to their capacities of extracellular electron transfer [44].

To obtain more detailed and accurate information beyond marker gene analysis, shotgun metagenomics was used to examine the anode microbial community (Fig. 5, Fig. S3-S6). In general, both analyses showed consistent results except abundance of *Geobacter* (Fig. 5B). Although fermenter *Bacteroides* and *Dysgonomonas* were still dominant in metagenomic analysis, *Geobacter* abundance (4–17%) were far higher than that of 16S rRNA gene results (~3.1%), especially in active harvesting scenarios of CH and PH, which had the highest abundance. Moreover, *Geobacter* abundance is positively correlated with current production (Fig. 1), indicating the direct contribution of this species in extracellular electron transfer. This selective process may be different from that by employing a control of anode potentials [12], because active harvesting simultaneously improved anode energy losses by reducing overpotential. More importantly, metagenomics enables accurate identification of the specific species of *Geobacter* (Fig. 5C, D). More than 12 *Geobacter* species were detected with high diversity, which is more comprehensive than that of a previous study based on the control of bioanode potential [11]. This study revealed a selective enrichment of only *Geobacter sulfurreducens*, and lower anode potential led to higher abundance of *G. sulfurreducens*. Our result also showed that there was

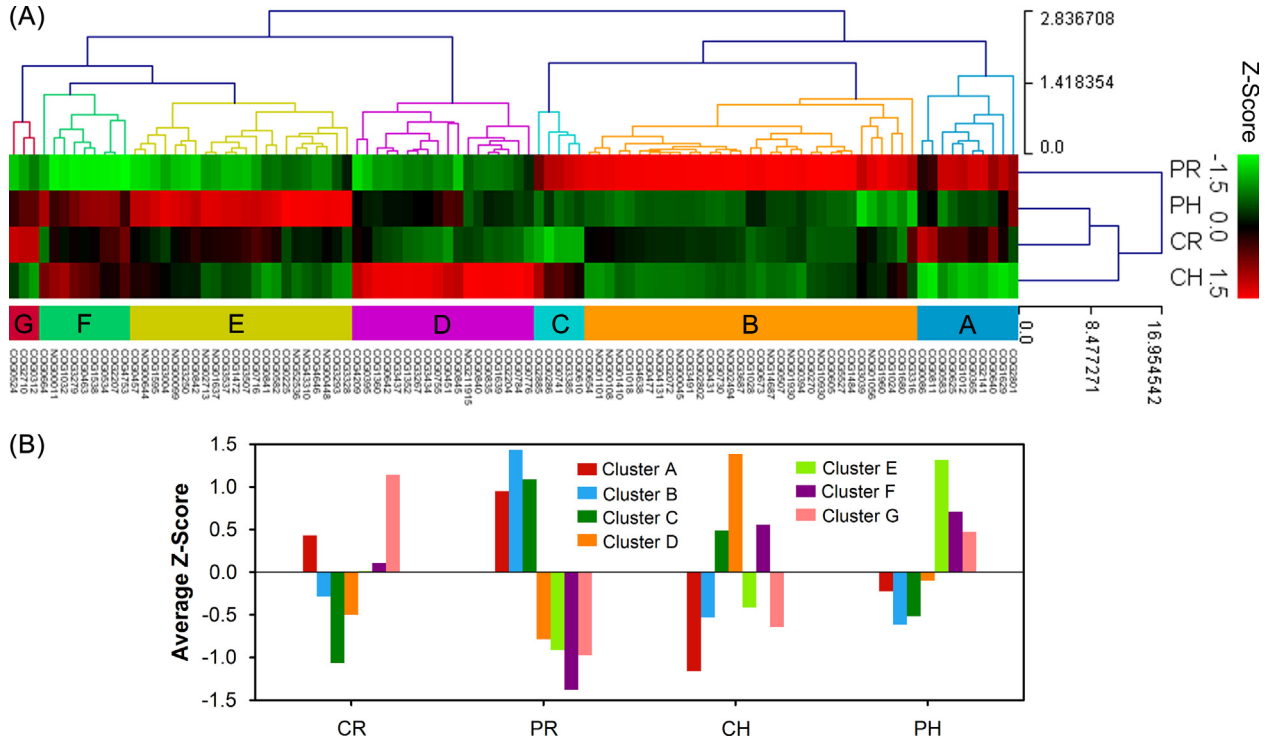

Fig. 6. (A) Clustering of the bioanode communities based on COG functional annotation of the genes. The relative abundance of the genes was performed a z-score normalization. (B) A total of seven gene clustering of A-G were observed across four communities under maximum current (CR) and power (PR) using resistor as well as maximum current (CH) and power (PH) using active energy harvesting circuit.

no obvious difference on the distribution of each species under four scenarios of energy harvesting, indicating an adjustment of EAB to the active harvesting is primarily due to physiological adaption, such as the increase of key enzyme expression (see data below). On the contrary, anode potential control showed a selection of particular *Geobacter* strains and species, such as *G. psychrophilus*, at a specific anode potential [45]. *Desulfovibrio desulfuricans* has been reported involved in direct extracellular electron transfer to the anode [46–48] and it accounted for a majority of *Desulfovibrio* population, which are more abundant in the passive harvesting systems. Their roles on current generation compared to *Geobacter* under different harvesting conditions will be an interesting topic to explore further.

Clusters of COG functional annotation of gene was used to visualize how the functional genes changed under different energy harvesting scenarios (Fig. 6). Cluster analysis show that PH and CR anode communities displayed a greater similarity and were well separated from PR and CH samples, consistent with PCoA results (Fig. 3A, D). A total of seven different gene clustering (A-G) were observed in overall functional profile. The CH community with the highest current production displayed a gene clustering D that has obviously higher abundance than that in other samples (Fig. 6B, orange bar). The genes in this group are majorly involved in cytochrome c, and binding-protein-dependent transport systems inner membrane component, which are generally responsible for direct extracellular electron transfer [49]. While genes involved in lipid transport and metabolism as well as replication, recombination and repair (group B, blue bar in Fig. 6B) were most abundant in PR with the lower electricity generation. The genes assigned into carbohydrate transport and metabolism as well as energy production and conversion (group E, green bar in Fig. 6B) had the highest abundance in PH with the highest power production.

3.5. Statistical analysis shows the correlation matrix between anode functional community and electrochemical performance

Although active harvesting using an electrical circuit has been observed to enhance MFC energy recovery from wastewater and be able to shape the both structure and function of electroactive community in MFCs (Figs. 1-6), a statistical analysis of these data, such as significance test, is needed to avoid a possibility that this observed effect occurred due to random errors. Table 1 shows a correlation matrix (coefficient and significance level) between the anode functional community parameters (e.g. midpoint potential, Shannon biodiversity index-H', abundance of *Geobacter* and *c*-type cytochrome genes) and electrochemical performance parameters (e.g. anode potential, power and current output, Coulombic efficiency, EAB activity showed as maximum anodic current on the CV). The most obvious relationship was that both current output and electroactive bacteria activity showed a strong positive correlation with the abundance of *Geobacter* and *c*-type cytochrome genes (COG) as well as Coulombic efficiency ($P < 0.01$), and a negative correlation with midpoint potential ($P < 0.001$) and biodiversity index. These statistical analyses solidly supported our observation and reveled for the first time that active harvesting significantly improved MFC performance by simultaneous enrichment of electroactive bacteria (EAB) and enhancement of EAB capability of extracellular electron transfer (increased gene abundance of c-type cytochromes) (Fig. 6 and S12). None of the previous studies associated with energy harvesting conducted microbiological investigation [6,13,15,16,50]. In our study, the anode potential is negatively correlated with power output (strong, $P < 0.01$) and current output (medium, $P < 0.01$). Most previous studies without active energy harvesting showed a positive correlation between potential and current production at least within a potential range [12,51,52]. Although the use of a higher anode potential improves the maximum current of MFC, more energy loss due to overpotential will occur on the anode. Compared to this, active harvesting can simultaneously enhance current generation while maintaining low energy loss.

4. Conclusions

Compared with using a resistor in MFCs without harvesting usable

Table 1
Correlation Matrix (Coefficient and Significance Level) between the anode potential (E_{anode}), power output (P), current output (I), Coulombic efficiency (CE), electroactive bacteria (EAB) activity, anode biofilm biodiversity (Shannon index, H'), and relative abundance of *Geobacter* sp. and *c*-type cytochrome genes (*c*-Cyt) determined from metagenomic sequences and corresponding functional annotation by COG pathways.

	E_{anode}	P	I	CE	EAB activity	$E_{midpoint}$	H'	*Geobacter*
P	**−0.874**	/						
	0.002[b]							
I	−0.441	−0.014	/					
	0.002[b]	0.927						
CE	−0.459	0.042	**0.913**	/				
	0.001[b]	0.777	**0.000**[c]					
EAB activity	−0.125	−0.331	**0.910**	**0.914**	/			
	0.396	0.022[a]	**0.000**[c]	**0.000**[c]				
$E_{midpoint}$	**0.692**	−0.342	**−0.870**	**−0.703**	**−0.609**	/		
	0.030[a]	0.017[a]	**0.004**[b]	**0.020**[a]	**0.002**[b]			
H'	0.387	−0.123	**−0.553**	**−0.826**	**−0.677**	0.290	/	
	0.138	0.650	**0.026**[a]	**0.006**[b]	**0.010**[a]	0.277		
Geobacter	−0.354	−0.105	**0.969**	**0.950**	**0.931**	**−0.783**	−0.672	/
	0.390	0.804	**0.000**[c]	**0.000**[c]	**0.000**[c]	**0.021**[a]	0.068	
c-Cyt (COG)	−0.120	−0.328	**0.818**	**0.918**	**0.998**	−0.585	**−0.712**	**0.961**
	0.776	0.428	**0.003**[b]	**0.001**[b]	**0.000**[c]	0.127	**0.048**[a]	**0.000**[c]

Correlation: Strong (positive, 0.5 to 1.0 or negative, −1.0 to −0.5), Medium (positive, 0.3 to 0.5 or negative, −0.5 to −0.3), Small (positive, 0.1 to 0.3 or negative, −0.3 to −0.1, None (positive, 0.0 to 0.1 or negative, −0.1 to 0). Sample number is 48 for all parameters except H' (16 samples) and relative abundance of *Geobacter* sp. and c-Cyt genes (4 samples).
Strong positive correlation with $P < 0.05$ was highlighted in bold.
[a] $P < 0.05$.
[b] $P < 0.01$.
[c] $P < 0.001$.

energy, this study showed that active energy harvesting using a tunable electrical circuit significantly enhanced electrical energy recovery from real wastewater in MFCs under maximum current or maximum power scenarios. More importantly, we for the first time revealed that this boosted performance was mainly due to an enhanced capability of electron transfer by electroactive microbiomes on the anode, which showed up a statistical increase of abundance in both electroactive bacteria *Geobacter* and c-type cytochrome genes associated with electron transfer under active harvesting. Metagenomics used in this study not only examined the structure of microbial community on the bioanode but also provided community function profiles. Previous studies in passive harvesting systems generally depended on the 16S rRNA gene sequencing, which couldn't provide information of community function. Moreover, our study showed that 16S rRNA gene method could underestimate the abundance of *Geobacter*, leading to an obscure conclusion. These results on reactor performance, electrochemical characterizations, microbial community and function, as well as statistical analysis provide a solid evidence that active harvesting is an effective approach to maximize MFC energy output. Further study could focus on the application of active harvesting to the other microbial electrochemical technologies.

Acknowledgements

We thank the financial support from CAPES (Science without Borders), the Office of Naval Research (Award N000141310901), the National Science Foundation (CBET 1510682), and the State Key Laboratory of Urban Water Resource and Environment.

Appendix A. Supplementary material

Supplementary data to this article can be found online at https://doi.org/10.1016/j.apenergy.2019.04.074.

References

[1] Logan BE, Wallack MJ, Kim K-Y, He W, Feng Y, Saikaly PE. Assessment of microbial fuel cell configurations and power densities. Environ Sci Technol Lett 2015;2:206–14.
[2] Wang H, Ren ZJ. A comprehensive review of microbial electrochemical systems as a platform technology. Biotechnol Adv 2013;31:1796–807.
[3] Lovley DR. Bug juice: harvesting electricity with microorganisms. Nat Rev Microbiol 2006;4:497–508.
[4] Wang H, Luo H, Fallgren PH, Jin S, Ren ZJ. Bioelectrochemical system platform for sustainable environmental remediation and energy generation. Biotechnol Adv 2015;33:317–34.
[5] Yang W, Kim K-Y, Saikaly P, Logan BE. The impact of new cathode materials relative to baseline performance of microbial fuel cells all with the same architecture and solution chemistry. Energy Environ Sci 2017;10:1025–33.
[6] Wang H, Park J-D, Ren ZJ. Practical energy harvesting for microbial fuel cells: a review. Environ Sci Technol 2015;49:3267–77.
[7] Del Pilar ARM, Zaiat M, Gonzalez ER, De Wever H, Pant D. Effect of the electric supply interruption on a microbial electrosynthesis system converting inorganic carbon into acetate. Bioresour Technol 2018;266:203–10.
[8] Rojas MdPA, Mateos R, Sotres A, Zaiat M, Gonzalez ER, Escapa A, et al. Microbial electrosynthesis (MES) from CO2 is resilient to fluctuations in renewable energy supply. Energy Convers Manag 2018;177:272–9.
[9] Logan BE, Hamelers B, Rozendal RA, Schrorder U, Keller J, Freguia S, et al. Microbial fuel cells: methodology and technology. Environ Sci Technol 2006;40:5181–92.
[10] Dennis PG, Virdis B, Vanwonterghem I, Hassan A, Hugenholtz P, Tyson GW, et al. Anode potential influences the structure and function of anodic electrode and electrolyte-associated microbiomes. Sci Rep 2016;6:39114.
[11] Torres CI, Krajmalnik-Brown R, Parameswaran P, Marcus AK, Wanger G, Gorby YA, et al. Selecting anode-respiring bacteria based on anode potential: phylogenetic, electrochemical, and microscopic characterization. Environ Sci Technol 2009;43:9519–24.
[12] Zhu X, Yates MD, Hatzell MC, Ananda Rao H, Saikaly PE, Logan BE. Microbial community composition is unaffected by anode potential. Environ Sci Technol 2014;48:1352–8.
[13] Wang H, Park J-D, Ren Z. Active energy harvesting from microbial fuel cells at the maximum power point without using resistors. Environ Sci Technol 2012;46:5247–52.
[14] Lobo FL, Wang X, Ren ZJ. Energy harvesting influences electrochemical performance of microbial fuel cells. J Power Sources 2017;356:356–64.
[15] Park J-D, Ren Z. High efficiency energy harvesting from microbial fuel cells using a synchronous boost converter. J Power Sources 2012;208:322–7.
[16] Alaraj M, Ren ZJ, Park J-D. Microbial fuel cell energy harvesting using synchronous flyback converter. J Power Sources 2014;247:636–42.
[17] Poretsky R, Rodriguez-R LM, Luo C, Tsementzi D, Konstantinidis KT. Strengths and limitations of 16S rRNA gene amplicon sequencing in revealing temporal microbial community dynamics. PLoS ONE 2014;9:e93827.
[18] Ranjan R, Rani A, Metwally A, McGee HS, Perkins DL. Analysis of the microbiome: advantages of whole genome shotgun versus 16S amplicon sequencing. Biochem Biophys Res Commun 2016;469:967–77.
[19] Cheng S, Liu H, Logan BE. Increased performance of single-chamber microbial fuel cells using an improved cathode structure. Electrochem Commun 2006;8:489–94.
[20] Park J-D, Ren Z. Hysteresis controller based maximum power point tracking energy harvesting system for microbial fuel cells. J Power Sources 2012;205:151–6.

[21] Lu L, Hou D, Fang Y, Huang Y, Ren ZJ. Nickel based catalysts for highly efficient H_2 evolution from wastewater in microbial electrolysis cells. Electrochim Acta 2016;206:381–7.
[22] Wang H, Ren Z, Park J-D. Power electronic converters for microbial fuel cell energy extraction: effects of inductance, duty ratio, and switching frequency. J Power Sources 2012;220:89–94.
[23] Wang X, Zhou L, Lu L, Lobo FL, Li N, Wang H, et al. Alternating current influences anaerobic electroactive biofilm activity. Environ Sci Technol 2016;50:9169–76.
[24] Chookaew T, Prasertsan P, Ren ZJ. Two-stage conversion of crude glycerol to energy using dark fermentation linked with microbial fuel cell or microbial electrolysis cell. N Biotechnol 2014;31:179–84.
[25] Caporaso JG, Kuczynski J, Stombaugh J, Bittinger K, Bushman FD, Costello EK, et al. QIIME allows analysis of high-throughput community sequencing data. Nat Methods 2010;7:335–6.
[26] Sun D, Cheng S, Zhang F, Logan BE. Current density reversibly alters metabolic spatial structure of exoelectrogenic anode biofilms. J Power Sources 2017;356:566–71.
[27] Sun D, Cheng S, Wang A, Li F, Logan BE, Cen K. Temporal-spatial changes in viabilities and electrochemical properties of anode biofilms. Environ Sci Technol 2015;49:5227–35.
[28] Lu G, Zhu Y, Lu L, Xu K, Wang H, Jin Y, et al. Iron-rich nanoparticle encapsulated, nitrogen doped porous carbon materials as efficient cathode electrocatalyst for microbial fuel cells. J Power Sources 2016;315:302–7.
[29] Freguia S. Organics Oxidation. In: Rabaey K, Angenent L, Schröder U, Keller J, editors. Bioelectrochemical Systems: From Extracellular Electron Transfer to Biotechnological Application. first ed.London, New York: IWA Publishing; 2009. p. 225–39.
[30] Liu Y, Kim H, Franklin RR, Bond DR. Linking spectral and electrochemical analysis to monitor c-type cytochrome redox status in living *Geobacter sulfurreducens* biofilms. ChemPhysChem 2011;12:2235–41.
[31] Si Ishii, Suzuki S, Norden-Krichmar TM, Phan T, Wanger G, Nealson KH, et al. Microbial population and functional dynamics associated with surface potential and carbon metabolism. ISME J 2014;8:963–78.
[32] Ying X, Guo K, Chen W, Gu Y, Shen D, Zhou Y, et al. The impact of electron donors and anode potentials on the anode-respiring bacteria community. Appl Microbiol Biotechnol 2017;101:7997–8005.
[33] Wang H, Qu Y, Da Li JJA, He W, Zhou X, Liu J, et al. Cascade degradation of organic matters in brewery wastewater using a continuous stirred microbial electrochemical reactor and analysis of microbial communities. Sci Rep 2016;6:27023.
[34] Miran W, Nawaz M, Kadam A, Shin S, Heo J, Jang J, et al. Microbial community structure in a dual chamber microbial fuel cell fed with brewery waste for azo dye degradation and electricity generation. Environ Sci Pollut Res 2015;22:13477–85.
[35] Wrighton KC, Agbo P, Warnecke F, Weber KA, Brodie EL, DeSantis TZ, et al. A novel ecological role of the Firmicutes identified in thermophilic microbial fuel cells. ISME J 2008;2:1146–56.
[36] Ren Z, Ward TE, Regan JM. Electricity production from cellulose in a microbial fuel cell using a defined binary culture. Environ Sci Technol 2007;41:4781–6.
[37] Lu L, Xing D, Ren N, Logan BE. Syntrophic interactions drive the hydrogen production from glucose at low temperature in microbial electrolysis cells. Bioresour Technol 2012;124:68–76.
[38] Yang Y, Xu M, Guo J, Sun G. Bacterial extracellular electron transfer in bioelectrochemical systems. Process Biochem 2012;47:1707–14.
[39] Kumar A, Hsu LH-H, Kavanagh P, Barrière F, Lens PN, Lapinsonnière L, et al. The ins and outs of microorganism–electrode electron transfer reactions. Nat Rev Chem 2017;1:0024.
[40] Sydow A, Krieg T, Mayer F, Schrader J, Holtmann D. Electroactive bacteria—molecular mechanisms and genetic tools. Appl Microbiol Biotechnol 2014;98:8481–95.
[41] Yu J, Park Y, Cho H, Chun J, Seon J, Cho S, et al. Variations of electron flux and microbial community in air-cathode microbial fuel cells fed with different substrates. Water Sci Technol 2012;66:748–53.
[42] Logan BE. Exoelectrogenic bacteria that power microbial fuel cells. Nat Rev Microbiol 2009;7:375–81.
[43] Hodgson DM, Smith A, Dahale S, Stratford JP, Li JV, Grüning A, et al. Segregation of the anodic microbial communities in a microbial fuel cell cascade. Front Microbiol 2016;7:699.
[44] Kiely PD, Call DF, Yates MD, Regan JM, Logan BE. Anodic biofilms in microbial fuel cells harbor low numbers of higher-power-producing bacteria than abundant genera. Appl Microbiol Biotechnol 2010;88:371–80.
[45] Commault AS, Lear G, Packer MA, Weld RJ. Influence of anode potentials on selection of Geobacter strains in microbial electrolysis cells. Bioresour Technol 2013;139:226–34.
[46] Fritz G, Griesshaber D, Seth O, Kroneck PM. Nonaheme cytochrome c, a new physiological electron acceptor for [Ni, Fe] hydrogenase in the sulfate-reducing bacterium Desulfovibrio desulfuricans Essex: primary sequence, molecular parameters, and redox properties. Biochemistry 2001;40:1317–24.
[47] Kang CS, Eaktasang N, Kwon D-Y, Kim HS. Enhanced current production by *Desulfovibrio desulfuricans* biofilm in a mediator-less microbial fuel cell. Bioresour Technol 2014;165:27–30.
[48] Wang K, Sheng Y, Cao H, Yan K, Zhang Y. Impact of applied current on sulfate-rich wastewater treatment and microbial biodiversity in the cathode chamber of microbial electrolysis cell (MEC) reactor. Chem Eng J 2017;307:150–8.
[49] Shi L, Dong H, Reguera G, Beyenal H, Lu A, Liu J, et al. Extracellular electron transfer mechanisms between microorganisms and minerals. Nat Rev Microbiol 2016;14:651–62.
[50] Degrenne N, Allard B, Buret F, Adami S-E, Labrousse D, Vollaire C, et al. A 140 mV self-starting 10 mW DC/DC converter for powering low-power electronic devices from low-voltage microbial fuel cells. J Low Power Electron 2012;8:485–97.
[51] Hou D, Lu L, Ren ZJ. Microbial fuel cells and osmotic membrane bioreactors have mutual benefits for wastewater treatment and energy production. Water Res 2016;98:183–9.
[52] Wagner RC, Call DF, Logan BE. Optimal set anode potentials vary in bioelectrochemical systems. Environ Sci Technol 2010;44:6036–41.